PCCP

PAPER

View Article Online
View Journal | View Issue

Cite this: *Phys. Chem. Chem. Phys.*, 2015, **17**, 30378

Dynamic atomic contributions to infrared intensities of fundamental bands

Arnaldo F. Silva, Wagner E. Richter, Adalberto B. M. S. Bassi and Roy E. Bruns*

Dynamic atomic intensity contributions to fundamental infrared intensities are defined as the scalar products of dipole moment derivative vectors for atomic displacements and the total dipole derivative vector of the normal mode. Intensities of functional group vibrations of the fluorochloromethanes can be estimated within 6.5 km mol^{-1} by displacing only the functional group atoms rather than all the atoms in the molecules. The asymmetric CF_2 stretching intensity, calculated to be 126.5 km mol^{-1} higher than the symmetric one, is accounted for by an 81.7 km mol^{-1} difference owing to the carbon atom displacement and 40.6 km mol^{-1} for both fluorine displacements. Within the Quantum Theory of Atoms in Molecules (QTAIM) model differences in atomic polarizations are found to be the most important for explaining the difference in these carbon dynamic intensity contributions. Carbon atom displacements almost completely account for the differences in the symmetric and asymmetric CCl_2 stretching intensities of dichloromethane, 103.9 of the total calculated value of 105.2 km mol^{-1}. Contrary to that found for the CF_2 vibrations intramolecular charge transfer provoked by the carbon atom displacement almost exclusively explains this difference. The very similar intensity values of the symmetric and asymmetric CH_2 stretching intensities in CH_2F_2 arise from nearly equal carbon and hydrogen atom contributions for these vibrations. All atomic contributions to the intensities for these vibrations in CH_2Cl_2 are very small. Sums of dynamic contributions of the individual intensities for all vibrational modes of the molecule are shown to be equal to mass weighted atomic effective charges that can be determined from atomic polar tensors evaluated from experimental infrared intensities and frequencies. Dynamic contributions for individual intensities can also be determined solely from experimental data.

Received 19th August 2015,
Accepted 16th October 2015

DOI: 10.1039/c5cp04949k

www.rsc.org/pccp

Introduction

Infrared intensities have been historically studied in spectroscopy mainly for extracting information about molecular electronic structures. Atomic charges, in particular, were widely used by vibrational spectroscopy researchers in many attempts to establish their relations with variations in molecular electronic structure. Many different partition models were developed over the years in order to extract charge information from the infrared spectrum, usually separating infrared intensities into dynamic and static contributions. Sorted by their formulation dates, some of the most successful include Equilibrium Charge–Charge Flux (ECCF),[1] the Charge–Charge Flux–Overlap (CCFO),[2] the Charge–Charge Flux–Overlap Modified (CCFOM)[3] and the Charge–Charge Flux–Dipole Flux (CCFDF)[4] model, developed within the physics of Bader's Quantum Theory of Atoms in Molecules (QTAIM).[5] Recently intensity results were expressed as a squared function of charge, charge flux and dipole flux terms.[6] Furthermore the analysis of the infrared intensities of hydrocarbons has led to a new interpretation of the CCFDF contributions in terms of intramolecular atomic charge transfer and counter polarization. The infrared intensities of the simple hydrocarbons containing sp^2 and sp^3 carbons were quantitatively accounted for by these contributions without the necessity of including a pure charge term. Among the hydrocarbons, the charge contribution is significant only for vibrations with sp carbons.[7] The CCFDF decomposition was also used to successfully interpret the infrared intensity enhancements of the water dimer[8] and trimer[9] in terms of atomic contributions.

As such this work on the halomethane intensities has two main objectives. First, a better understanding of dynamic atomic intensity contributions for individual vibrations is sought and their potential usefulness for electronic structure analysis is determined by examining atomic parameters for this family of molecules ranging from the nonpolar methane to the very polar fluoro- and chlorofluoromethanes. Second, the sum of these atomic contributions over all the molecular fundamental modes provides an expression for the intensity sum analogous to Crawford's G sum rule.[10] The relation of these dynamic atomic intensity sum contributions with the parameters of the G sum rule, the atomic effective charges, is also presented. Indeed Person and Kubulat[11,12]

Instituto de Química, Universidade Estadual de Campinas, CP 6154, CEP 13.083-970, Campinas, São Paulo, Brazil. E-mail: bruns@iqm.unicamp.br

have suggested the calculation of atomic contributions previously and showed that the sum of these contributions are related to the atomic effective charges of the water molecule. The use of QTAIM leads to an interpretation of the infrared atomic effective charges and the closely related mean dipole moment derivatives, sometimes called GAPT charges,[13] in terms of well-defined electronic structure changes. Furthermore the atomic effective charges can also be evaluated from atomic polar tensors and are linearly related to the electronegativity of a substituent atom whereas the carbon atomic effective charges are related to the average electronegativity of their substituents.[14] Here the dependence of the dynamic atomic intensity sum contributions on electronegativity is also investigated.

Calculations and methodology

Computational details

The first step of our work was to choose which experimental infrared intensities would be used as references, since there are several measurements from different research groups. Therefore three criteria were used to select the experimental data that would be used: (1) the intensities must have been measured for all the fundamental bands of the molecule, (2) error estimates from scattering of Beer's law plots must have been reported and (3) in the case of hydrogen-containing molecules, intensity measurements and error estimates must have been made for at least two isotopomers. For the fluoro- and chloromethanes isotopomeric intensity data permits some validation of the quality of measured values by means of the G intensity sum rule[10] and the isotopic invariance property of atomic polar tensor elements.[15,16]

The methane data were taken from four different experimental studies.[17–20] The methyl fluoride data are from Overend and coworkers,[21] methylene fluoride from Kondo *et al.*[22] and fluoroform from Kim and King.[23] The tetrafluoromethane intensities used here are averages of results obtained by three research groups.[24–26] The methyl chloride values are averages of results from Russell *et al.*,[21] Dickson *et al.*[27] and Saeki and associates.[28] The methylene chloride results are from Saeki and Tanabe[29] whereas the chloroform data are averages of results from two research groups.[30,31] For carbon tetrachloride results were taken from ref. 32. Average values from several references were taken for CF_3Cl,[33,34] CF_2Cl_2[35–37] and $CFCl_3$.[34,35,38,39,40] Comparisons of theoretical values calculated at the QCISD/cc-pVTZ level with their experimental values resulted in rms errors of 14.8, 22.4 and 22.2 km mol^{-1} respectively for the fluoro-, chloro- and fluorochloromethanes. This can be consider excellent agreement as the intensity values for these molecules range from almost zero to 414 km mol^{-1}.

The molecular geometries were optimized using Gaussian03 program[41] on a 64 Opteron workstation which also generated the wave functions to be used by the MORPHY98 program.[42] The optimized geometries were then used to obtain the fundamental infrared intensities and polar tensors also using Gaussian03. The QTAIM multipoles were calculated through MORPHY98 by integrating the equilibrium and distorted wave functions generated by Gaussian03. As in our previous work[43] refined carbon parameters from MORPHY98 were corrected using the multipole moments of the terminal atoms, charge sum neutrality and the molecular dipole moment expression. Distorted geometries were generated by displacing each atom by 0.01 Å along each Cartesian axis in both the positive and negative directions. Each one of the $6N$ (N being the number of atoms) distorted geometries and the equilibrium geometry has its own set of AIM atomic multipoles. As will be demonstrated later accurate intensity values can be obtained by displacing only the characteristic group of atoms. The atomic charges and atomic dipoles are then used by the PLACZEK[44] program to calculate the molecular dipole moment derivatives and atomic polar tensors.

Methodology

The molecular polar tensor[15,16]

$$\mathbf{P}_X = [\mathbf{P}_X^{(1)} \vdots \mathbf{P}_X^{(2)} \vdots \cdots \vdots \mathbf{P}_X^{(N)}] \quad (1)$$

is a juxposition of 3 × 3 atomic polar tensors having $\partial p_\sigma/\partial \nu_j$ elements where $\sigma, \nu = x, y, z, j = 1,\ldots, N$, and N is the number of atoms in the molecule. As the polar tensor elements depend on the molecular orientation in the Cartesian coordinate system, roto-translational invariant polar tensor quantities have been used for the interpretation of polar tensor results in terms of molecular electronic structure. The mean dipole moment derivative, for $j = 1,\ldots, N$,

$$\bar{\mathrm{P}}^{(j)} = \frac{1}{3}\mathrm{Tr}\left(\mathbf{P}_X^{(j)}\right) \quad (2)$$

and the closely related atomic effective charge

$$\chi_j{}^2 = \frac{1}{3}\mathrm{Tr}\left[\mathbf{P}_X^{(j)}\mathbf{P}_X^{(j)^{\mathrm{T}}}\right] \quad (3)$$

are most often found in the literature. These invariants have been shown to be related to atomic electronegativities[11] and ionization energies of core electrons through Siegbahn's simple potential model.[45] The atomic effective charges are related to the sum of the intensities, $\sum A_k$, by the G sum rule[10]

$$\sum_{k=1}^{3N-6} A_k + \Omega = K\sum_{j=1}^{N}\frac{\chi_j{}^2}{M_j} \quad (4)$$

where K is a constant, Ω, a rotational correction and M_j the mass of the jth atom. As such the molecular intensity sum can be expressed as a sum of atomic terms involving the squares of the dipole moment derivatives with respect to atomic Cartesian coordinates. Here search is carried out to find atomic invariants for individual intensities that might be useful for their interpretation in terms of molecular electronic structure changes during vibrations.

Within the QTAIM model, for $\sigma, \nu = x, y, z$, and $i, j = 1,\ldots, N$, the polar tensor elements are given by

$$\frac{\partial p_\sigma}{\partial \nu_j} = q_j^0 + \sum_{i=1}^{N}\sigma_i^0\frac{\partial q_i}{\partial \nu_j} + \sum_{i=1}^{N}\frac{\partial m_{i,\sigma}}{\partial \nu_j}, \quad \text{for } \sigma = \nu \quad (5)$$

and

$$\frac{\partial p_\sigma}{\partial \nu_j} = \sum_{i=1}^{N}\sigma_i^0\frac{\partial q_i}{\partial \nu_j} + \sum_{i=1}^{N}\frac{\partial m_{i,\sigma}}{\partial \nu_j}, \quad \text{for } \sigma \neq \nu \quad (6)$$

where q_j^0 is the equilibrium atomic charge on the displaced jth atom and σ_i^0 is the equilibrium atomic coordinate. The second term of eqn (5) and first term of eqn (6) involve atomic charge rearrangements and the last terms correspond to changes in the atomic dipoles of all the atoms owing to this displacement. As such the polar tensor elements contain dynamic atomic contributions to the atomic dipole moment derivatives. On transforming to normal coordinates, for $k = 1,\ldots, 3N - 6$, $\sigma = x, y, z$,

$$\frac{\partial p_\sigma}{\partial Q_k} = \sum_{j=1}^{N}\left[\sum_{\nu=x,y,z}\left(\frac{\partial p_\sigma}{\partial \nu_j}\right)\left(\frac{\partial \nu_j}{\partial Q_k}\right)\right] = \sum_{j=1}^{N}\left(\frac{\partial p_\sigma}{\partial Q_k}\right)^{(j)} \quad (7)$$

where Cartesian coordinates of the same atom are grouped together in dynamic atomic contributions. As such, for $\sigma = x, y, z$, $j = 1,\ldots, N$

$$\left(\frac{\partial p_\sigma}{\partial Q_k}\right)^{(j)} = q_j^0\left(\frac{\partial \nu_j}{\partial Q_k}\right) + \sum_{\nu=x,y,z}^{N}\left(\sum_{i=1}^{N}\frac{\partial[q_i + m_{i,\sigma}]}{\partial \nu_j}\right)\left(\frac{\partial \nu_j}{\partial Q_k}\right) \quad (8)$$

This derivative includes equilibrium charge, charge transfer and polarization contributions owing to displacement of the jth atom in the kth normal coordinate. In general, atomic displacements along one of the Cartesian axes can provoke changes in the charge transfer and polarization contributions in all Cartesian directions while it only provides nonzero charge contributions in the direction of the displaced atom. So, the last term describes change tendencies in charge transfer and polarization related to displacements of the jth atom along the three Cartesian directions, each of which is weighted by its importance in the kth normal coordinate.

Alternatively, each dynamic atomic contribution can be expressed as contributions from charge movement, charge rearrangement and atomic dipole change contributions,

$$\left(\frac{\partial p_\sigma}{\partial Q_k}\right)^{(j)} = \left(\frac{\partial p_\sigma}{\partial Q_k}\right)_{\mathrm{C}}^{(j)} + \left(\frac{\partial p_\sigma}{\partial Q_k}\right)_{\mathrm{CF}}^{(j)} + \left(\frac{\partial p_\sigma}{\partial Q_k}\right)_{\mathrm{DF}}^{(j)}. \quad (9)$$

The above atomic dipole derivative contributions will be shown to be useful for simplifying interpretations of changes in electronic structures for molecular vibrations.

As the intensity is proportional to the square of dipole moment derivative, summing over all the fundamental vibrational modes of the molecule with dipole moment changes along the σ direction, for $\sigma = x, y, z$, results in

$$\sum_{k=1}^{3N-6} A_{k,\sigma} = K\sum_{k=1}^{3N-6}\left(\frac{\partial p_\sigma}{\partial Q_k}\right)\left(\frac{\partial p_\sigma}{\partial Q_k}\right) \quad (10)$$

$$\sum_{k=1}^{3N-6} A_{k,\sigma} = K\sum_{k=1}^{3N-6}\left\{\sum_{j=1}^{N}\left[\sum_{\nu=x,y,z}\left(\frac{\partial p_\sigma}{\partial \nu_j}\right)\left(\frac{\partial \nu_j}{\partial Q_k}\right)\right]\left[\sum_{\nu'=x,y,z}\left(\frac{\partial p_\sigma}{\partial \nu_j'}\right)\left(\frac{\partial \nu_j'}{\partial Q_k}\right)\right]\right\}. \quad (11)$$

This gives the intensity sum owing to dipole moment changes along the σ-axis. The total intensity sum is the sum of these contributions for each Cartesian direction. The sum in eqn (11) over the remaining six degrees of freedom is the same as the trace of the matrix in eqn (30) of the paper by Person and Newton[16] giving the rotational correction term of eqn (4).

Now, the norm of the vector $\frac{\partial \vec{p}}{\partial Q_k}$ is proportional to the square root of the intensity and it can involve dipole changes in all three Cartesian coordinate directions,

$$\frac{\partial \vec{p}}{\partial Q_k} = \left(\frac{\partial p_x}{\partial Q_k}\right)^{(1)}\vec{i} + \left(\frac{\partial p_y}{\partial Q_k}\right)^{(1)}\vec{j} + \left(\frac{\partial p_z}{\partial Q_k}\right)^{(1)}\vec{k} + \cdots + \left(\frac{\partial p_x}{\partial Q_k}\right)^{(N)}\vec{i} + \left(\frac{\partial p_y}{\partial Q_k}\right)^{(N)}\vec{j} + \left(\frac{\partial p_z}{\partial Q_k}\right)^{(N)}\vec{k} \quad (12)$$

Through eqn (7),

$$A_k = K\left(\frac{\partial \vec{p}}{\partial Q_k}\right)\cdot\left(\frac{\partial \vec{p}}{\partial Q_k}\right) = K\left[\sum_{j=1}^{N}\left(\frac{\partial \vec{p}^{(j)}}{\partial Q_k}\right)\cdot\left(\frac{\partial \vec{p}}{\partial Q_k}\right)\right] \quad (13)$$

$$A_k = A_k^{(1)} + A_k^{(2)} + \cdots + A_k^{(N)} \quad (14)$$

As such, a dynamic atomic intensity contribution to the fundamental infrared intensity can be defined as the scalar product of the dipole moment derivative vector for an atomic displacement by the total dipole derivative vector of the normal mode. Thus, the intensity of the kth normal mode is simply a sum of the scalar products of the dynamic atomic dipole moment derivatives of all atoms in the molecule by the dipole moment derivative of that normal mode. Within QTAIM the directions of the atomic contributions are determined by the sizes of the Cartesian components represented by eqn (8) in terms of equilibrium charge displacement, charge transfer and dipolar polarization.

Summing over the $3N - 6$ normal coordinates

$$\sum_{k=1}^{3N-6} A_k = \sum_{j=1}^{N}\left(\sum_{k=1}^{3N-6}\frac{\partial \vec{p}^{(j)}}{\partial Q_k}\right)\cdot\frac{\partial \vec{p}}{\partial Q_k} \quad (15)$$

Now, comparing eqn (15) with the G-sum rule shown in eqn (4),

$$\sum_{k=1}^{3N-6}\frac{\partial \vec{p}^{(j)}}{\partial Q_k}\cdot\frac{\partial \vec{p}}{\partial Q_k} = K\left(\frac{\chi_j^{\,2}}{M_j}\right) \quad (16)$$

As such, for molecules with no permanent dipole moment (for which Ω is null), the square of the atomic effective charge weighted by its inverse mass is just the sum over all normal modes of scalar products of the jth atomic dipole moment derivative of the normal mode by the total dipole moment derivative vector of that normal mode. For molecules with a permanent dipole moment, Ω can be recovered by also summing over the six translational and rotational modes in eqn (11).

Results

Intensity analysis with dynamic atomic contributions

Characteristic group vibrational frequencies have been used for many years in qualitative analysis being useful for understanding similarities in electronic structure changes on vibrational

displacements. Although there has been some activity working with characteristic group intensities[46] their use has been limited perhaps owing to the much larger variations observed for their intensities compared with their frequencies values.

Dynamic contributions of the atoms making up the characteristic group can be used to simplify the intensity analysis. The total dipole moment derivative of a molecular vibration is assumed to be adequately estimated by only the dynamic atomic dipole moment derivative contributions of the atoms composing the functional group. Then the important dynamic contributions are analyzed in terms of equilibrium charge displacement, charge transfer and polarization effects. Table 1 contains the dynamic atomic intensity contributions for 67 normal modes of the fluorochloromethanes. Each normal mode is identified by its characteristic group atoms with the type of vibration, stretching or deformation. Included in the last line for each molecule are values for the atomic intensity sum contributions. Fig. 1 contains a graph of the functional group dynamic intensity contributions plotted against the total calculated intensities for most of the normal modes in Table 1. All vibrations are included in Fig. 1 except for those of CH_4, CF_4 and CCl_4 as well as half-dozen others with indefinite band assignments. As can be seen in this figure the agreement is excellent. The rms error is 6.2 km mol^{-1} compared with an average intensity of 64.2 km mol^{-1}.

Their usefulness is demonstrated by analyzing differences in the absorption intensities of symmetric and asymmetric stretching intensities. It has long been known that asymmetric band intensities are larger than symmetric ones. For C–H vibrations of the difluoro- and dichloroethylenes and the fluorochloromethanes the average asymmetric intensity, 26.6 km mol^{-1}, is slightly higher than the symmetric one of 20.4 km mol^{-1}. This difference is much more pronounced for the C–F stretching vibrations with the asymmetric average, 232.4 km mol^{-1}, being almost double the symmetric one, 143.6 km mol^{-1}. In addition, the average value for the asymmetric C–Cl stretching vibrations,

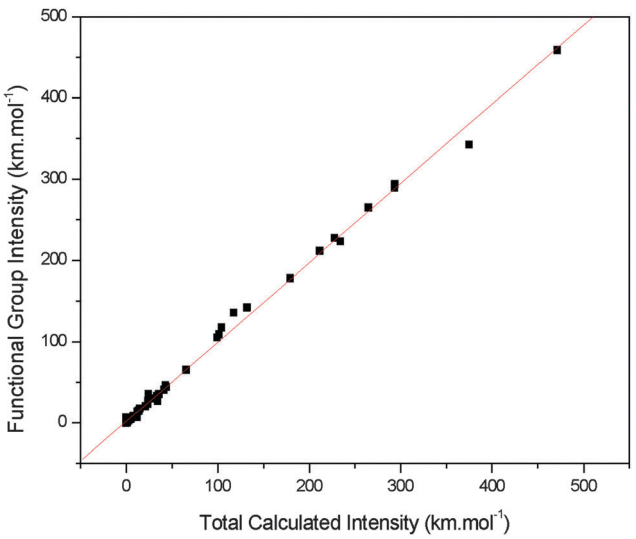

Fig. 1 Sums of the dynamic atomic contributions of the functional group atoms *vs.* the total intensities of the fluorochloromethanes.

Table 1 Dynamic atomic intensity contributions calculated at the QCISD/cc-pVTZ level for the fundamental intensities of the fluorochloromethanes (km mol^{-1})

			Atomic contributions					
Molecule	Vibration		C(1)	H(2)	H(3)	H(4)	H(5)	Total
CH_4	νC–H	Q_3	0.3	1.0	15.5	5.8	0.6	23.2
	νC–H	Q_3	0.3	6.5	1.4	11.1	3.9	23.2
	νC–H	Q_3	0.3	10.0	0.2	0.2	12.6	23.3
	δH–C–H	Q_4	−0.2	1.7	2.1	3.3	3.3	10.2
	δH–C–H	Q_4	−0.2	3.2	3.1	1.2	3.0	10.3
	δH–C–H	Q_4	−0.2	3.0	2.7	3.3	1.5	10.3
Total			0.3	25.4	25.0	24.9	24.9	100.5
			C(1)	F(2)	H(3)	H(4)	H(5)	Total
CH_3F	νC–H	Q_1	6.7	−0.3	7.3	7.8	7.8	29.3
	δH–C–H	Q_2	5.3	−0.8	−0.5	−0.5	−0.5	3.0
	νC–F	Q_3	59.7	42.3	−0.9	−0.9	−0.9	99.3
	νC–H	Q_4	6.5	0.0	17.0	3.2	6.4	33.1
	νC–H	Q_4	6.7	0.0	0.4	15.7	12.4	35.2
	δH–C–H	Q_5	−1.2	0.1	1.9	0.9	0.9	2.6
	δH–C–H	Q_5	−1.2	0.1	0.5	1.6	1.6	2.6
	—	Q_6	1.9	0.5	0.0	−0.3	−0.4	1.7
	—	Q_6	1.9	0.5	−0.5	−0.2	−0.1	1.6
Total			86.3	42.4	25.2	27.3	27.2	208.4
			C(1)	F(2)	F(3)	H(4)	H(5)	Total
CH_2F_2	νC–H	Q_1	13.7	−0.1	−0.1	15.1	15.1	43.7
	δH–C–H	Q_2	3.5	−0.1	−0.1	−1.0	−1.0	1.3
	νC–F	Q_3	69.8	17.7	17.7	−2.0	−2.0	101.2
	δF–C–F	Q_4	8.0	−1.1	−1.1	−0.2	−0.2	5.4
	νC–H	Q_6	14.6	0.0	0.0	13.1	13.1	40.8
	—	Q_7	17.4	1.6	1.6	0.1	0.1	20.8
	δH–C–H	Q_8	25.3	−0.9	−0.9	−0.1	−0.1	23.3
	νC–F	Q_9	151.5	38.0	38.0	0.1	0.1	227.7
Total			303.8	55.3	55.3	25.1	25.1	464.5
			C(1)	H(2)	F(3)	F(4)	F(5)	Total
CHF_3	νC–H	Q_1	18.7	16.6	0.0	0.0	0.0	35.3
	νC–F	Q_2	84.6	−6.6	8.7	8.7	8.7	104.1
	δF–C–F	Q_3	17.8	−1.4	−0.6	−0.6	−0.6	14.6
	δH–C–F	Q_4	61.4	−0.1	1.1	1.6	1.5	65.5
	δH–C–F	Q_4	61.3	−0.1	1.7	1.2	1.3	65.4
	νC–F	Q_5	189.5	0.1	1.3	37.8	36.2	264.9
	νC–F	Q_5	189.4	0.1	48.9	12.4	14.0	264.8
	δF–C–F	Q_6	6.8	0.0	−4.9	0.6	0.5	3.0
	δF–C–F	Q_6	6.8	0.0	2.4	−3.1	−3.1	3.0
Total			636.3	8.6	58.6	58.6	58.5	820.6
			C(1)	F(2)	F(3)	F(4)	F(5)	Total
CF_4	νC–F	Q_3	330.7	3.2	3.2	31.7	38.2	407.0
	νC–F	Q_3	330.2	6.3	35.6	20.2	14.2	406.5
	νC–F	Q_3	330.7	47.8	18.4	5.3	4.8	407.0
	δF–C–F	Q_4	12.7	−9.5	0.9	0.8	0.8	5.7
	δF–C–F	Q_4	12.7	2.2	−8.3	−0.4	−0.4	5.8
	δF–C–F	Q_4	12.7	2.2	2.2	−5.6	−5.6	5.9
Total			1029.7	52.2	52.0	52.0	52.0	1237.9
			C(1)	Cl(2)	H(3)	H(4)	H(5)	Total
CH_3Cl	νC–H	Q_1	4.1	0.0	6.4	6.4	6.4	23.3
	δH–C–H	Q_2	7.5	−0.5	2.3	2.3	2.3	13.9
	νC–Cl	Q_3	22.7	6.6	−1.7	−1.7	−1.7	24.2
	νC–H	Q_4	0.9	0.0	2.9	0.2	2.0	6.0
	νC–H	Q_4	0.9	0.0	0.5	3.2	1.4	6.0
	δH–C–H	Q_5	−0.6	0.0	4.0	1.0	0.4	4.8
	δH–C–H	Q_5	−0.6	0.0	−0.4	2.6	3.2	4.8
	—	Q_6	−0.6	−0.2	1.0	0.9	0.9	2.0
	—	Q_6	−0.6	−0.2	0.9	1.0	0.9	2.0
Total			33.7	5.7	15.9	15.9	15.8	87.0

Table 1 (*continued*)

			C(1)	Cl(2)	Cl(3)	H(4)	H(5)	Total
CH_2Cl_2	νC–H	Q_1	2.3	0.0	0.0	2.9	2.9	8.1
	δH–C–H	Q_2	0.0	0.0	0.0	0.0	0.0	0.0
	νC–Cl	Q_3	10.3	1.4	1.4	−0.4	−0.4	12.3
	δCl–C–Cl	Q_4	0.9	−0.2	−0.2	0.0	0.0	0.5
	νC–H	Q_6	0.1	0.0	0.0	0.0	0.0	0.1
	—	Q_7	−0.7	−0.1	−0.1	0.9	0.9	0.9
	δH–C–H	Q_8	23.5	−0.9	−0.9	10.3	10.3	42.3
	νC–Cl	Q_9	103.9	11.3	11.3	−4.5	−4.5	117.5
Total			140.3	11.5	11.5	9.2	9.2	181.7

			C(1)	H(2)	Cl(3)	Cl(4)	Cl(5)	Total
$CHCl_3$	νC—H	Q_1	−0.1	0.4	0.0	0.0	0.0	0.3
	νC—Cl	Q_2	3.9	0.5	0.3	0.3	0.3	5.3
	δCl—C—Cl	Q_3	0.5	0.1	−0.1	−0.1	−0.1	0.4
	δH—C—Cl	Q_4	14.3	10.1	−0.7	−0.1	−0.1	23.5
	δH—C—Cl	Q_4	14.3	10.2	0.1	−0.5	−0.5	23.5
	νC—Cl	Q_5	115.6	−5.2	0.4	10.6	10.6	132.0
	νC—Cl	Q_5	115.6	−5.2	14.0	3.8	3.8	131.9
	—	Q_6	0.8	−0.1	−0.6	0.0	0.0	0.1
	—	Q_6	0.8	−0.1	0.2	−0.4	−0.4	0.1
Total			265.7	10.7	13.6	13.6	13.6	317.1

			C(1)	Cl(2)	Cl(3)	Cl(4)	Cl(5)	Total
CCl_4	νC–Cl	Q_3	119.3	0.4	0.4	7.7	9.6	137.4
	νC–Cl	Q_3	119.3	1.1	9.0	4.9	3.1	137.4
	νC–Cl	Q_3	115.7	12.1	0.6	1.0	0.9	137.4
	δCl–C–Cl	Q_4	−0.1	0.1	0.0	0.0	0.0	0.0
	δCl–C–Cl	Q_4	−0.1	0.0	0.1	0.0	0.0	0.0
	δCl–C–Cl	Q_4	−0.1	0.0	0.0	0.0	0.0	0.0
Total			354.0	13.7	10.1	13.6	13.6	412.2

			C(1)	F(2)	Cl(3)	Cl(4)	Cl(5)	Total
CCl_3F	νC–F	Q_1	123.9	54.9	0.2	0.2	0.2	179.4
	νC–Cl	Q_2	5.3	−5.0	0.4	0.4	0.4	1.5
	δCl–C–Cl	Q_3	−0.6	0.6	0.0	0.0	0.0	0.0
	νC–Cl	Q_4	207.1	5.6	0.6	10.5	10.5	234.3
	νC–Cl	Q_4	207.0	5.6	13.7	3.9	3.9	234.1
	δF–C–Cl	Q_5	0.3	0.5	−0.5	−0.1	−0.1	0.1
	δF–C–Cl	Q_5	0.3	0.5	0.0	−0.4	−0.4	0.0
	δF–C–Cl	Q_5	−0.2	0.1	0.1	0.0	0.0	0.0
	δF–C–Cl	Q_5	−0.2	0.1	−0.1	0.1	0.1	0.0
			542.9	62.9	14.4	14.6	14.6	649.4

			C(1)	F(2)	F(3)	Cl(4)	Cl(5)	Total
CCl_2F_2	νC–F	Q_1	220.5	35.3	35.3	1.1	1.1	293.3
	νC–Cl	Q_2	0.2	0.5	0.5	−0.5	−0.5	0.2
	δCl–C–Cl	Q_3	22.2	−6.7	−6.8	1.4	1.4	11.5
	δCl–C–Cl	Q_4	−0.4	0.2	0.2	0.0	0.0	0.0
	νC–F	Q_6	154.8	28.3	28.3	0.1	0.1	211.6
	δF–C–F	Q_7	0.0	−0.1	−0.1	0.1	0.1	0.0
	νC–Cl	Q_8	335.0	8.4	8.4	11.7	11.7	375.2
	δF–C–F	Q_9	3.6	−1.6	−1.6	0.1	0.1	0.6
Total			735.9	64.3	64.2	14.0	14.0	892.4

			C(1)	Cl(2)	F(3)	F(4)	F(5)	Total
$CClF_3$	νC–F	Q_1	384.9	6.3	25.9	27.0	27.0	471.1
	νC–Cl	Q_2	48.8	4.3	−6.3	−6.3	−6.3	34.2
	δF–C–F	Q_3	0.0	0.1	0.0	0.0	0.0	0.1
	νC–F	Q_4	227.6	0.2	41.7	10.3	13.9	293.7
	νC–F	Q_4	227.9	0.2	2.2	33.7	30.0	294.0
	δF–C–F	Q_5	7.6	0.1	1.7	−3.4	−3.5	2.5
	δF–C–F	Q_5	7.5	0.1	−5.2	0.0	0.1	2.5
	δCl–C–F	Q_6	0.5	0.0	−0.6	0.1	0.1	0.1
	δCl–C–F	Q_6	0.5	0.0	−0.1	−0.2	−0.2	0.0
Total			905.3	11.3	59.3	61.2	61.1	1098.2

166.6 km mol^{-1}, is more than four times the average for the symmetric ones, 36.2 km mol^{-1}. The C–F and C–Cl averages include data for the X_2CY (X = F, Cl; Y = O, S) molecules.

Table 2 contains values of the dynamic atomic contributions to the intensities of the symmetric and asymmetric stretching vibrations of the fluoro- and chloromethanes. It is easily seen that the electronic structure changes resulting in the infrared intensities are largely localized in the characteristic functional group. The first five columns with numerical entries in this table contain the dynamic atomic intensity contributions of each atom in the molecule. Atoms not belonging to the vibrational characteristic group have intensity contributions of less than about 5% of the total intensities.

As examples, electronic structure changes corresponding to the symmetric and asymmetric stretching intensities of difluoro- and dichloromethane are explained in detail. As can be seen in Table 2 dynamic contributions from the CF_2 or CCl_2 atoms explain almost all of the total intensity values for the CF and C–Cl stretching modes. For CH_2F_2, contributions from carbon and fluorine sum to 227.5 km mol^{-1} for the asymmetric stretch compared with a total value of 227.7 km mol^{-1}. For the symmetric stretch these contributions are 105.2 km mol^{-1} compared to 101.2 km mol^{-1}. So, the difference in the dynamic contributions of the CF_2 functional group atoms for these two vibrations is 122.3 km mol^{-1} compared to the total calculated difference of 126.5 km mol^{-1}. Furthermore, the dynamic carbon contribution difference for these vibrations is 81.7 km mol^{-1} or 65% of the total intensity difference. The two dynamic fluorine contributions account for 40.6 km mol^{-1} or 32% of this difference. The hydrogen contributions explain a remaining 3%. Therefore, analysis of the carbon and fluorine dynamic contributions provides an assessment of the electronic structure origins of a large portion of the intensity difference between the CH_2F_2 symmetric and asymmetric CF_2 stretches. The experimental values show an even larger difference between these intensities, 269.1 and 60.6 km mol^{-1} with the asymmetric intensity value being about four times the symmetric one.

The CF_2 group forms a local plane in the molecule that can be represented as in Fig. 2. The dynamic carbon atom contribution of the functional group atoms of the symmetric stretching dipole derivative can be expressed as ($z_c^0 = 0$)

$$\frac{\partial p_z}{\partial Q_{\mathrm{sym}}} \approx \left\{ q_c^0 + \left(\frac{\partial q_{F_1}}{\partial z_C}\right) R_{CF}^0 \cos\left(\frac{\alpha}{2}\right) + \left(\frac{\partial q_{F_2}}{\partial z_C}\right) R_{CF}^0 \cos\left(\frac{\alpha}{2}\right) + \frac{\partial m_{C,z}}{\partial z_C} + \frac{\partial m_{F_1,z}}{\partial z_C} + \frac{\partial m_{F_2,z}}{\partial z_C} \right\} \frac{\partial z_C}{\partial Q_{\mathrm{sym}}}$$

$$\frac{\partial z_C}{\partial Q_{\mathrm{sym}}} \approx [1.314 + (-0.184)(2.554)(0.580) + (-0.184)(2.554)(0.580) + 0.355 - 0.103 - 0.103](0.205)$$

where R_{CF}^0, α and q_c^0 are the equilibrium C–F bond length, F–C–F angle and equilibrium carbon atomic charge, respectively. Hydrogen atom terms of the dynamic carbon contribution have not been specifically detailed in this equation as they are not important in explaining the intensity difference.

Table 2 Dynamic atomic intensity contributions calculated at the QCISD/cc-pVTZ level for the symmetric and asymmetric stretching intensities of the fluorochloromethanes (km mol^{-1})

Molecule	Vibration	Atom (1)	Atom (2)	Atom (3)	Atom (4)	Atom (5)	Total
CH_3F		(C)	(F)	(H)	(H)	(H)	—
	C–H sym	6.7	−0.3	7.3	7.8	7.8	29.3
	C–H asym	6.5	0.0	17.0	3.2	6.4	33.1
CH_2F_2		(C)	(F)	(F)	(H)	(H)	—
	C–H sym	13.7	−0.1	−0.1	15.1	15.1	43.7
	C–H asym	14.6	0.0	0.0	13.1	13.1	40.8
		(C)	(F)	(F)	(H)	(H)	
	C–F sym	69.8	17.7	17.7	−2.0	−2.0	101.2
	C–F asym	151.5	38.0	38.0	0.1	0.1	227.7
CHF_3		(C)	(H)	(F)	(F)	(F)	—
	C–F sym	84.6	−6.6	8.7	8.7	8.7	104.1
	C–F asym	189.5	0.1	1.3	37.8	36.2	264.9
CH_2Cl_2		(C)	(Cl)	(Cl)	(H)	(H)	—
	C–H sym	2.3	0.0	0.0	2.9	2.9	8.1
	C–H asym	0.1	0.0	0.0	0.0	0.0	0.1
		(C)	(Cl)	(Cl)	(H)	(H)	—
	C–Cl sym	10.3	1.4	1.4	−0.4	−0.4	12.3
	C–Cl asym	103.9	11.3	11.3	−4.5	−4.5	117.5
$CHCl_3$		(C)	(H)	(Cl)	(Cl)	(Cl)	—
	C–Cl sym	3.9	0.5	0.3	0.3	0.3	5.3
	C–Cl asym	115.6	−5.2	14.0	3.8	3.8	131.9

The asymmetric stretch is given by a similar expression ($y_c^0 = 0$)

$$\frac{\partial p_y}{\partial Q_{\text{asym}}} \approx \left\{ q_c^0 - \left(\frac{\partial q_{F_1}}{\partial y_C}\right) R_{CF}^0 \sin\left(\frac{\alpha}{2}\right) + \left(\frac{\partial q_{F_2}}{\partial y_C}\right) R_{CF}^0 \sin\left(\frac{\alpha}{2}\right) + \frac{\partial m_{C,y}}{\partial y_C} + \frac{\partial m_{F_1,y}}{\partial y_C} + \frac{\partial m_{F_2,y}}{\partial y_C} \right\} \frac{\partial y_C}{\partial Q_{\text{asym}}}$$

$$\frac{\partial p_y}{\partial Q_{\text{asym}}} \approx [1.314 - (+0.189)(2.554)(0.812) + (-0.189)(2.554)(0.812) + 0.657 + 0.204 + 0.204](0.214)$$

In terms of the charge displacement, charge transfer and counter polarization contributions

$$\frac{\partial p_z}{\partial Q_{\text{sym}}} \approx 0.269 - 0.112 + 0.031 = 0.188 \text{ au}$$

and

$$\frac{\partial p_y}{\partial Q_{\text{asym}}} \approx 0.281 - 0.168 + 0.228 = 0.341 \text{ au}$$

The results of this simplified CF_2 group model correspond to 34.5 km mol^{-1} for the symmetric and 113.4 km mol^{-1} for the asymmetric stretch. Their difference of 78.9 km mol^{-1} is close to the difference in the dynamic atomic carbon atom contributions of 81.7 km mol^{-1} in Table 2 for these vibrations. The small difference can be attributed to the effects of charge transfer and polarizations of the hydrogen atoms as the carbon atom is displaced.

The charge displacement contributions are almost the same for both normal coordinate derivatives. The negative charge transfer contribution has a somewhat larger magnitude for the asymmetric stretch than the symmetric one even though the

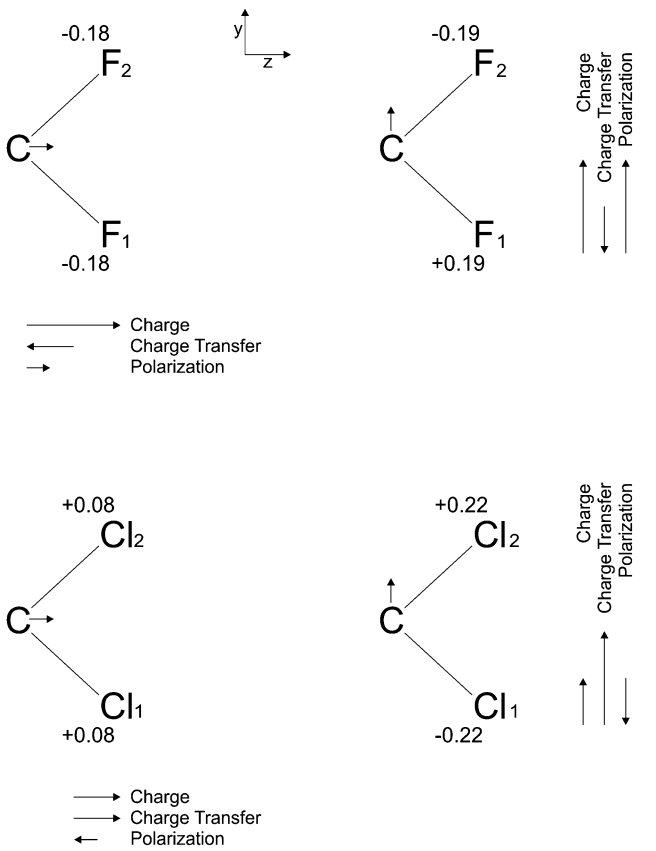

Fig. 2 QTAIM charge, charge transfer and polarization contributions for the dynamic carbon contribution for the symmetric and asymmetric stretching intensities of CH_2F_2 and CH_2Cl_2. the numbers given for the atoms are values of the charge transfer derivatives owing to the carbon atom displacements.

magnitudes of the charge derivatives are almost the same. The origin of this difference owes to the larger distance of the charge transfer along y for the asymmetric stretch compared with the one along z for the symmetric stretch owing to F–C–F angle which is greater than 90°. The charge transfer contribution is of opposite sign to the counter polarization term as found for most vibrations. The largest difference occurs for the counter polarization. Although the charge transfer term for the asymmetric stretch tends to decrease the dipole moment derivative more than for the symmetric stretch it is more than compensated by the counter polarization term that is about seven times larger for the asymmetric stretch relative to the symmetric one.

These functional group dipole moment derivative contributions are shown in Fig. 2. The charge contribution vectors are parallel to the direction of the displaced carbon atom and are about the same size for these two vibrations. The charge transfer vectors are of opposite direction indicating that the fluorine atoms in the direction of the displaced carbon atom become more negatively charged. Finally, the counter polarization vectors are of opposite sense to the charge transfer ones being very large for the asymmetric stretch and much smaller for the symmetric one.

The calculated asymmetric C–Cl stretching intensity for the CCl_2 group is almost ten times the symmetric one, 117.5 km mol^{-1} compared with 12.3 km mol^{-1}. The CCl_2 group contributions sum to 13.1 km mol^{-1} for the symmetric stretch and 126.5 km mol^{-1} for the asymmetric one. Both values accurately estimate the total calculated intensities. Indeed the experimental asymmetric intensity of 95 km mol^{-1} is even more than ten times the experimental symmetric intensity value of 8.0 km mol^{-1}.

The charge displacement, charge transfer and counter polarization contributions for these vibrations are

$$\frac{\partial p_z}{\partial Q_{\mathrm{sym}}} \approx 0.058 + 0.065 - 0.016 = 0.107 \text{ au}$$

and

$$\frac{\partial p_y}{\partial Q_{\mathrm{asym}}} \approx 0.058 + 0.275 - 0.040 = 0.293 \text{ au}$$

These values correspond to 11.2 and 83.7 km mol^{-1} in good agreement with the 10.3 and 103.9 km mol^{-1} dynamic carbon intensity contributions in Table 1. Therefore, the total intensity difference calculated for these vibrations of 105.2 km mol^{-1} is largely accounted for by the difference in the dynamic carbon contributions of 93.6 km mol^{-1} (see Table 2) of which 72.5 km mol^{-1} is estimated from the above equations.

As for the CF_2 vibrations, the charge contributions are the same for both derivatives. The charge transfer contribution clearly dominates the asymmetric stretching contributions being 0.210 au larger than the value for the symmetric one. Contrary to the behavior observed for the CF_2 vibrations the counter polarizations are more similar in magnitude with a difference of just 0.024 au. As shown in Fig. 2b this large difference has its origin in the magnitudes of the carbon charge derivatives, 0.22 e for the asymmetric stretch and only 0.08 e for the symmetric stretch, in contrast to what was found for the CF_2 stretches where they are similar, as shown in Fig. 2. Interestingly the carbon charge derivatives for the CCl_2 vibrations are opposite the CF_2 ones for both the symmetric and asymmetric stretches.

The calculated CHF_3 asymmetric stretching intensity is 160.8 km mol^{-1} greater than the symmetric one compared with a difference of 104.9 km mol^{-1} for the carbon dynamic contributions in Table 2. The changes in polarizations for these two stretches are larger than the charge transfer difference and account for 72.1 km mol^{-1}. As for the CF_2 vibrations in CH_2F_2, the equilibrium charge displacements are about the same for both vibrations. The fluorine dynamic contributions are also important and are 49.2 km mol^{-1} larger for the asymmetric stretch.

The carbon dynamic contribution for the asymmetric stretch is 111.7 km mol^{-1} larger than the symmetric stretch of $CHCl_3$ and accounts for most of the 126.6 km mol^{-1} difference in the total calculated intensities. This difference is principally due to a charge transfer contribution that is 83.7 km mol^{-1} larger for the asymmetric stretch. The equilibrium charge and polarization contributions are much smaller as they were for the CCl_2 stretching vibrations.

The calculated intensities of the symmetric and asymmetric CH_2 stretching vibrations of CH_2F_2 are almost the same for stretching modes, 43.7 and 40.8 km mol^{-1}. The CH_2 functional group contributions are 43.9 and 40.8 km mol^{-1}, respectively, in excellent agreement with the theoretical values. This compares with experimental values of 26.7 and 41.6 km mol^{-1}.

The carbon and hydrogen dynamic contributions are almost the same for these stretching motions. The symmetric stretching intensity is a little higher than the asymmetric one owing to its slightly larger hydrogen dynamic contribution, 15.1 km mol^{-1} for each hydrogen, compared with 13.1 km mol^{-1}. The carbon contributions are about the same, 13.7 and 14.6 km mol^{-1}, the smaller value corresponding to the symmetric stretch. Decomposition of these values shows that the individual charge, charge transfer and polarization contributions are also very similar for both vibrations.

The experimental and calculated intensities for the CH_2 stretching vibrations are in good agreement for CH_2Cl_2. For the symmetric mode, these values are 6.9 and 8.1 km mol^{-1}, respectively, and for the asymmetric one, 0.0 and 0.1 km mol^{-1}. This difference for the calculated intensities is accounted for by carbon and hydrogen atom contributions of 2.3 and 2.9 km mol^{-1}, respectively, for the symmetric stretch while they are only 0.1 and 0.0 km mol^{-1} for the asymmetric one.

The above discussion for CH_2F_2 and CH_2Cl_2 is summarized in Fig. 3. The sizes of the atomic contributions are given in bar graphs for all the intensities except the CH_2 stretches of CH_2Cl_2 that are very small. The thin bars below the ones for atomic contributions represent total intensity values.

Dynamic atomic contributions to intensity sums

Table 3 contains the atomic contributions to the infrared intensity sums for the fluorochloromethanes. As one can see the contributions for the central carbon atom varies sharply,

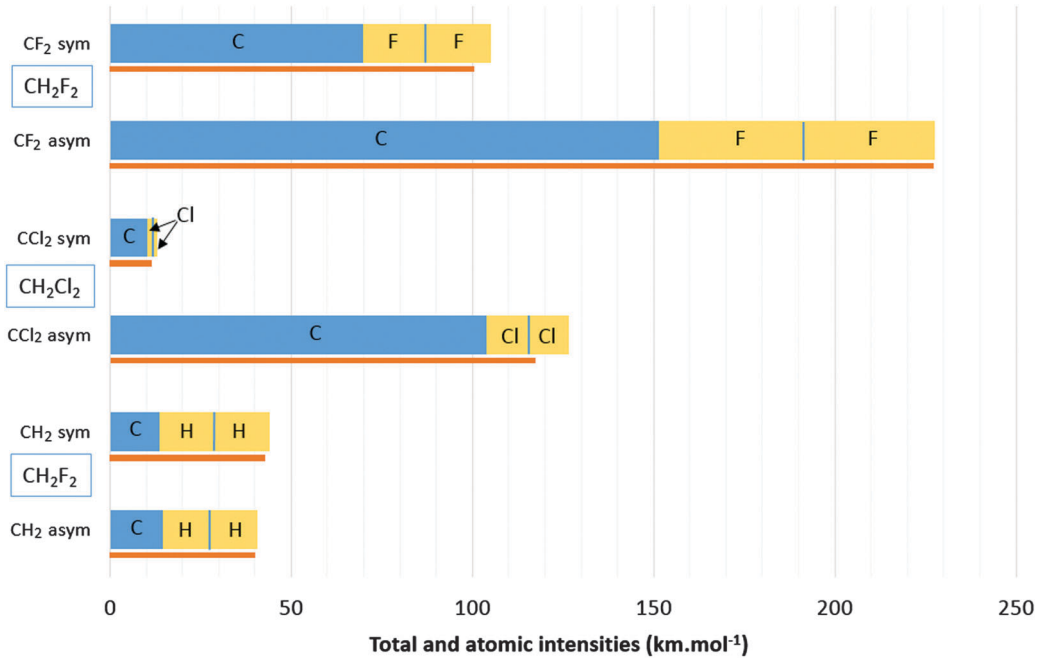

Fig. 3 Bar graphs showing the dynamic atomic contributions for the symmetric and asymmetric CF, CCl and CH stretches of CH_2F_2 and CH_2Cl_2. the thin bars below the dynamic atomic contributions represent the total infrared intensities.

ranging from 0.3 to 1029.7 km mol^{-1}. The highest value is the carbon atom contribution for CF_4 and the lowest value is found in CH_4. It is also worth mentioning that the largest difference between atomic QTAIM charges is also found for CF_4 (C; 2.8 *e* and F; −0.7 *e*), whereas the atomic charges are all close to zero in CH_4.

The dynamic atomic intensity sum contributions of terminal atoms do not vary quite as much as the carbon atom values. The atomic contributions for the hydrogen atoms range from 8.5 to 26.6 km mol^{-1}, the values for the chlorine atoms from 5.9 to 14.7 km mol^{-1} and those fluorine from 42.7 to 63.8 km mol^{-1}. This observation is consistent with the transferability of polar tensor related parameters for the terminal atoms relative to the carbons in the fluorochloromethanes observed previously by our group.[47] Even though these dynamic atomic contributions for the central carbon atom are not transferable among the fluorochloromethanes as might be expected, they appear to be related to the electronegativities of the terminal atoms bonded to it.

Based on observations of experimental results for polar tensor roto-translational invariants with behaviors similar to those described above, and the fact that the sum of all the fundamental intensities of a molecule can be expressed as a sum of atomic contributions as in the G-sum rule of eqn (4), an empirical model was proposed 25 years ago for the halomethanes.[14] It contains two basic assumptions: (1) the carbon atom intensity contributions in the halomethanes are proportional to the average electronegativity of the substituent halogen atoms and (2) the halogen atomic intensity contributions are proportional to their own electronegativities.

The first column of Table 3 contains electronegativity model estimates of the carbon contributions for the fluorochloromethanes,

Table 3 Atomic contributions to the sum of the fundamental infrared intensities of the fluorochloromethanes calculated at the QCISD/cc-pVTZ level and from the electronegativity model

Molecule	C (exp)	C	H	Cl	F	Total
CH_4	5.1	0.3	25.1	—	—	100.5
CH_3F	97.9	86.3	26.6	—	42.7	208.8
CH_2F_2	307.1	303.8	25.1	—	55.3	464.5
CHF_3	632.8	636.3	8.5	—	58.3	820.6
CF_4	1073.8	1029.7	—	—	51.9	1237.9
CH_3Cl	31.6	33.7	15.8	5.9	—	87.0
CH_2Cl_2	81.1	140.3	9.3	11.5	—	181.7
$CHCl_3$	153.1	265.7	10.9	13.6	—	317.1
CCl_4	246.4	354.0	—	12.9	—	412.2
CCl_3F	398.3	542.9	—	14.7	62.9	649.4
CCl_2F_2	586.5	735.9	—	14.1	63.8	892.4
$CClF_3$	811.0	905.3	—	11.4	60.7	1098.2
$\bar{x}$	—	—	17.3	12	56.5	—
Electro. model	—	—	18.1	8.0	56.4	—

determined from only experimental data and the last line has the average values for the terminal atom contributions. The next four columns contain dynamic atomic contributions to the intensity sum determined at the QCISD/cc-pVTZ level.

Fig. 4 shows a graph of both the QTAIM and electronegativity model atomic intensity sum contributions against the electronegativities. Minus signs have been assigned to the halogen substituent atoms since they clearly draw electron density from the carbon atoms. The fluoromethane atomic intensity sum contributions from the QCISD/cc-pVTZ QTAIM calculations and the electronegativity model results determined completely from experimental intensity data are in excellent agreement with an rms error of only 20.6 km mol^{-1}, or about 2% of the intensity variation. Most of this difference can be attributed

to the 14.8 km mol^{-1} root mean square difference between the calculated and experimental intensities. The chloro- and fluorochloromethanes show larger deviations from the electronegativity model values, the size of the deviations increasing for carbon atoms with more chlorine substituents. This might have been anticipated as the chlorine atoms are more polarizable than the fluorines that would cause deviations from a model based solely on electronegativity. Furthermore the averages of the QTAIM estimates for hydrogen, fluorine and chlorine atoms are 17.3, 56.5 and 12.0 km mol^{-1}, respectively, in excellent agreement with the 18.1, 56.4 and 8.0 km mol^{-1} obtained using experimental intensity values and assuming transferability of the halogens atoms as done in the electronegativity model.

Fig. 5 shows a graph of the dynamic contributions as a function of mass-weighted squares of effective charges of eqn (3) and (4) for all the atoms investigated here. The linear plot is almost perfect and the slope of this line is 2915.2 ± 10.4 km mol^{-1} which is the constant used to transform effective charge values in units of e^2 amu^{-1} to km mol^{-1}. The intercept is zero within the estimated error. Experimental values obtained from atomic polar tensors are given in Table 4 along with the QCISD/cc-pVTZ values and are highly correlated. Included in Table 4 are the zero flux equilibrium charges. The difference between the equilibrium charge and the effective charge values is determined by the charge transfer and polarization terms in eqn (8). As can be seen in Table 4, the sum of the charge transfer and polarization contributions have substantial sizes although the charge contributions are usually much larger. This hinders attempts to obtain accurate atomic charge estimates from infrared intensities.

Zero flux atomic charge values for the carbon atoms in the fluoromethanes are larger than their effective charges whereas they are smaller for the chloromethanes. As might be expected based on this observation, the carbon atomic charge value in CCl_3F is smaller than the effective charge value but it is larger in $CClF_3$. The difference is smaller in CCl_2F_2. As such the sum of the charge transfer and polarization contributions on carbon

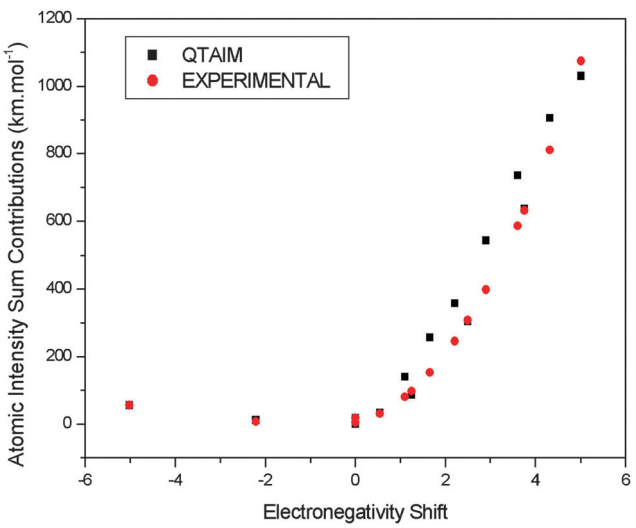

Fig. 4 Atomic intensity sum contributions determined from the QTAIM calculations and from the electronegativity model *vs.* the relative electronegativities of the fluorochloromethane atoms.

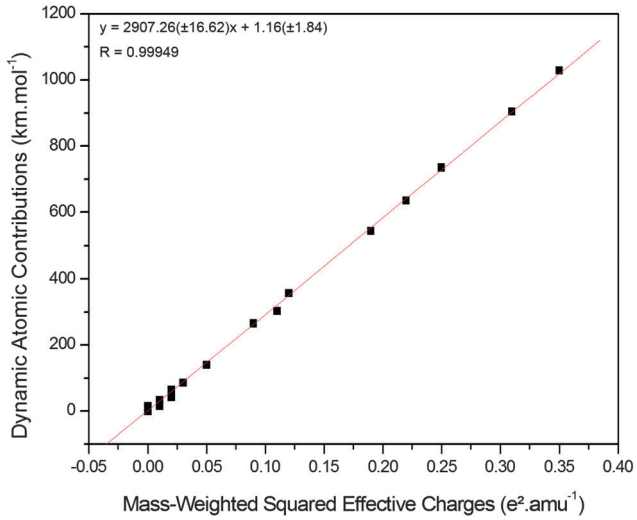

Fig. 5 Graph of the dynamic atomic intensity contributions of the fluorochloromethane atoms determined from QCISD/cc-pVTZ calculations against the mass-weighted squared effective charges determined from polar tensors at the same quantum level.

Table 4 Calculated QTAIM zero flux charges and effective charges at the QCISD/cc-pVTZ level, experimental effective charge values and dynamic atomic contributions for the fluorochloromethanes

			χ_α (*e*)		
Molecule	Atom	q_{ZF} (*e*)	Experimental	QCISD	DAC (km mol^{-1})
CH_4	C	0.013	0.016	0.000	0.1
	H	−0.003	0.054	0.082	24.9
CH_3F	C	0.650	0.606	0.632	86.2
	H	0.016	0.096	0.100	27.2
	F	−0.699	0.581	0.566	42.6
CH_2F_2	C	1.314	1.059	1.156	303.6
	H	0.046	0.079	0.082	25.1
	F	−0.703	0.574	0.603	55.3
CHF_3	C	2.021	1.546	1.627	635.7
	H	0.091	0.043	0.058	8.17
	F	−0.704	0.591	0.608	58.5
CF_4	C	2.786	2.051	2.055	1028.7
	F	−0.696	0.547	0.580	52.0
CH_3Cl	C	0.140	0.363	0.387	33.7
	H	0.044	0.074	0.082	5.9
	Cl	−0.271	0.301	0.306	15.9
CH_2Cl_2	C	0.255	0.676	0.772	140.3
	H	0.087	0.052	0.058	9.3
	Cl	−0.214	0.335	0.370	11.6
$CHCl_3$	C	0.363	0.940	1.047	265.6
	H	0.124	0.048	0.058	10.4
	Cl	−0.163	0.373	0.396	13.6
CCl_4	C	0.466	1.043	1.211	357.5
	Cl	−0.117	0.322	0.404	13.7
CCl_3F	C	1.051	1.354	1.492	542.6
	F	−0.680	0.608	0.640	62.8
	Cl	−0.124	0.428	0.416	14.6
CCl_2F_2	C	1.636	1.649	1.737	735.4
	F	−0.687	0.661	0.645	64.1
	Cl	−0.131	0.353	0.408	14.0
$CClF_3$	C	2.211	2.058	1.928	904.6
	F	−0.692	0.695	0.624	60.7
	Cl	−0.135	0.204	0.361	11.3

seems to depend on whether the substituent atom is fluorine or chlorine. The sizes of the fluorine zero flux charges are greater than those of the effective charge showing that the charge transfer and polarization effects partially cancel the charge effect on the intensities. On the other hand, they are smaller for chlorine showing that this sum reinforces the charge effect on the intensities.

Concluding remarks

Dynamic atomic contributions of both dipole moment derivatives and intensities have already been useful for the interpretation of hydrogen bonding intensity enhancements in the water dimer[8] and trimer.[9] We showed that intensity enhancement on hydrogen bonding for the water dimer can almost be completely accounted for by the intensity contribution of the hydrogen bridge atom. The intensity enhancement by the bridge atom contribution is calculated to be 145 km mol^{-1} whereas the total calculated enhancement is almost the same, 149 km mol^{-1} (experimental enhancement value of 141 km mol^{-1}). This may be closely connected to the hydrogen bond energy stabilization that has been found to be largely localized in the dimer coulomb and exchange integrals involving the bridge hydrogen and oxygen atoms compared with those integrals in the monomer molecules.[48] As the bridge hydrogen has much greater vibrational amplitude than the oxygen atom for the symmetric stretching mode the corresponding intensity enhancement shows up in the atomic hydrogen intensity contribution. So the bridge hydrogen contribution to the dipole moment derivative seems to be closely related to the hydrogen bonding stabilization energy in the water dimer.

Atomic dipole moment derivative contributions could lead to a fundamental understanding of the correlation between the enthalpies of hydrogen bond formation and the square root of infrared intensity enhancements that have been reported in the literature for many complexes in solution phase.[49] For the water trimer the hydrogen bridge atom contributions account for 99% of the total intensity of the two strongest symmetric stretches. Large portions of the hydrogen bond intensity enhancements in the HF dimer, 321 km mol^{-1}, and HF:H_2O complex, 592 km mol^{-1}, are accounted for by the 237 and 576 km mol^{-1} enhancements calculated for their bridge hydrogen atoms.[50] So these atomic contributions can be expected to simplify the analysis of these enhancements by localizing the regions where the important changes take place.

Dynamic atomic contributions to dipole moment derivatives, defined in eqn (7) and (8), should be useful to estimate infrared fundamental intensities They are vectorial parameters and intensities depend on both their magnitudes and directions. Transference of these atomic derivatives for some terminal atoms could work reasonably well but this will not be adequate for central atoms. Our approach will be to use characteristic substituent shift models[51] proposed by our group sometime ago. This model works accurately for the intensities of the X_2CY (X = F, Cl, Br; Y = O, S) molecules. The six experimental fundamental intensities of Cl_2CS were estimated almost within experimental error using only the polar tensors from F_2CO, Cl_2CO and F_2CS determined from experimental intensities.[51,52] In the 2004 reference we have reported 31 characteristic substituent shift relationships for the experimental mean dipole moment derivatives of carbon atoms. Furthermore one can expect many more of these relations to work for carbon atoms as many characteristic shifts have been reported for carbon 1*s* core ionization energies that are linearly related to carbon mean dipole moment derivatives by Siegbahn's simple potential model.[53]

Acknowledgements

W. E. R. thanks CNPq (Conselho Nacional de Desenvolvimento Científico e Tecnológico, grant 140711/2013-9) for graduate student fellowship. A. F. S. thanks FAPESP (Fundação de Amparo à Pesquisa do Estado de São Paulo, grant 2014/21241-9) for postdoc research fellowship and R. E. B. thanks CNPq for a research fellowship. We are also grateful to FAPESP for partial financial support of this work (grant 09/09678-4).

References

1 J. C. Decius, *J. Mol. Spectrosc.*, 1975, **57**, 384.
2 W. T. King and G. B. Mast, *J. Phys. Chem.*, 1976, **80**, 2521.
3 M. Gussoni, M. N. Ramos, C. Castiglioni and G. Zerbi, *Chem. Phys. Lett.*, 1987, **142**, 515.
4 R. L. A. Haiduke and R. E. Bruns, *J. Phys. Chem. A*, 2005, **109**, 2680.
5 R. F. W. Bader, *Atoms in Molecules. A Quantum Theory*, Clarendon Press, Oxford, 1990.
6 A. F. Silva, W. E. Richter, H. G. C. Meneses, S. H. D. M. Faria and R. E. Bruns, *J. Phys. Chem. A*, 2012, **116**, 8238.
7 A. F. Silva, W. E. Richter, H. G. C. Meneses and R. E. Bruns, *Phys. Chem. Chem. Phys.*, 2014, **16**, 23224.
8 A. F. Silva, W. E. Richter, L. A. Terrabuio, R. L. A. Haiduke and R. E. Bruns, *J. Chem. Phys.*, 2014, **140**, 084306.
9 A. F. Silva, W. E. Richter and R. E. Bruns, *Chem. Phys. Lett.*, 2014, **610–611**, 14.
10 B. L. Crawford, Jr., *J. Chem. Phys.*, 1952, **20**, 977.
11 W. B. Person and K. Kubulat, *J. Mol. Struct.*, 1988, **173**, 357.
12 W. B. Person and K. Kubulat, *J. Mol. Struct.*, 1990, **224**, 225.
13 J. Cioslovski, *J. Am. Chem. Soc.*, 1989, **111**, 8333.
14 B. B. Neto and R. E. Bruns, *J. Phys. Chem.*, 1990, **94**, 1764.
15 J. F. Biarge, J. Herranz and J. Morcillo, *An. R. Soc. Esp. Fis. Quim., Ser. A*, 1961, **A57**, 81.
16 W. B. Person and J. H. Newton, *J. Chem. Phys.*, 1974, **61**, 1040.
17 J. Heicklen, *Spectrochim. Acta, Part A*, 1961, **17**, 201.
18 J. H. G. Bode and W. M. A. Smit, *J. Phys. Chem.*, 1980, **84**, 198.
19 S. Saëki, M. Mizuno and K. Kondo, *Spectrochim. Acta, Part A*, 1976, **32**, 403.
20 K. Kim, *J. Quant. Spectrosc. Radiat. Transfer*, 1987, **37**, 107.

21 J. W. Russell, C. D. Needham and J. Overend, *J. Chem. Phys.*, 1966, **45**, 3383.
22 S. Kondo, T. Nakanaga and S. Saeki, *J. Chem. Phys.*, 1980, **73**, 5409.
23 K. Kim and W. T. King, *J. Chem. Phys.*, 1980, **73**, 5591.
24 S. Saeki and K. Tanabe, *Spectrochim. Acta, Part A*, 1969, **25**, 1325.
25 B. J. Schurin, *Chem. Phys.*, 1959, **30**, 1.
26 C. M. Roehl, D. Boglu and G. K. Moortgat, *Geophys. Res. Lett.*, 1995, **22**, 815.
27 A. D. Dickson, I. M. Mills, Jr. and B. Crawford, *J. Chem. Phys.*, 1957, **27**, 445.
28 S. Kondo, Y. Koga, T. Nakanaga and S. Saeki, *Bull. Chem. Soc. Jpn.*, 1983, **56**, 416.
29 S. Saeki and K. Tanabe, *Spectrochim. Acta, Part A*, 1969, **25**, 1325.
30 K. Tanabe and S. Saeki, *Spectrochim. Acta, Part A*, 1970, **26**, 1469.
31 K. Kim and W. T. King, *J. Chem. Phys.*, 1984, **80**, 978.
32 K. Tanabe and S. Saeki, *Spectrochim. Acta, Part A*, 1970, **26**, 1469.
33 W. B. Person, S. K. Rudys and J. H. Newton, *J. Phys. Chem.*, 1975, **79**, 2525.
34 W. G. Golden, D. Horner and J. Overend, *J. Chem. Phys.*, 1978, **68**, 964.
35 P. Varanasi and F. K. Ko, *J. Quant. Spectrosc. Radiat. Transfer*, 1977, **17**, 385.
36 P. Varanasi and S. Chudmani, *J. Quant. Spectrosc. Radiat. Transfer*, 1988, **39**, 193.
37 J. Morcillo, L. J. Zamarano and J. M. V. Heredia, *Spectrochim. Acta, Part A*, 1966, **22**, 1969.
38 Z. Li and P. Varanasi, *J. Quant. Spectrosc. Radiat. Transfer*, 1994, **52**, 137.
39 R. Names, P. M. Silvaggio and R. W. Boese, *J. Quant. Spectrosc. Radiat. Transfer*, 1980, **23**, 211.
40 A. Goldman, F. S. Bonomo and D. G. Murcray, *Ap. Opt.*, 1976, **15**, 2305.
41 M. J. Frisch, G. W. Trucks, H. B. Schlegel, G. E. Scuseria, M. A. Robb, J. R. Cheeseman, J. A. Montgomery Jr., T. Vreven, K. N. Kudin, J. C. Burant, J. M. Millam, S. S. Iyengar, J. Tomasi, V. Barone, B. Mennucci, M. Cossi, G. Scalmani, N. Rega, G. A. Petersson, H. Nakatsuji, M. Hada, M. Ehara, K. Toyota, R. Fukuda, J. Hasegawa, M. Ishida, T. Nakajima, Y. Honda, O. Kitao, H. Nakai, M. Klene, X. Li, J. E. Knox, H. P. Hratchian, J. B. Cross, V. Bakken, C. Adamo, J. Jaramillo, R. Gomperts, R. E. Stratmann, O. Yazyev, A. J. Austin, R. Cammi, C. Pomelli, J. W. Ochterski, P. Y. Ayala, K. Morokuma, G. A. Voth, P. Salvador, J. J. Dannenberg, V. G. Zakrzewski, S. Dapprich, A. D. Daniels, M. C. Strain, O. Farkas, D. K. Malick, A. D. Rabuck, K. Raghavachari, J. B. Foresman, J. V. Ortiz, Q. Cui, A. G. Baboul, S. Clifford, J. Cioslowski, B. B. Stefanov, G. Liu, A. Liashenko, P. Piskorz, I. Komaromi, R. L. Martin, D. J. Fox, T. Keith, M. A. Al–Laham, C. Y. Peng, A. Nanayakkara, M. Challacombe, P. M. W. Gill, B. G. Johnson, W. Chen, M. W. Wong, C. Gonzalez and J. A. Pople, *Gaussian 03, Revision D.02*, Gaussian, Inc., Wallington CT, 2004.
42 MORPHY98, a program written by P. L. A. Popelier with a contribution from R. G. A. Bone, UMIST, Manchester, England, EU 1998.
43 A. F. Silva, J. V. da Silva, Jr., R. L. A. Haiduke and R. E. Bruns, *J. Phys. Chem. A*, 2011, **115**, 12572.
44 J. V. da Silva, Jr., L. N. Vidal, P. A. M. Vazquez and R. E. Bruns, *Int. J. Quantum Chem.*, 2010, **110**, 2029.
45 P. H. Guadagnini, A. E. Oliveira, R. E. Bruns and B. B. Neto, *J. Am. Chem. Soc.*, 1997, **119**, 4224.
46 D. Hadzi, in *Infra-red Spectroscopy and molecular structure*, ed. M. Davies, Elsevier, Amsterdam, 1963.
47 M. N. Ramos, B. Barros Neto and R. E. Bruns, *J. Phys. Chem.*, 1985, **89**, 4979.
48 M. Garcia-Revilla, E. Francisco, P. A. Popelier and A. M. Pendás, *ChemPhysChem*, 2013, **14**, 1211.
49 A. V. Iogansen, *Spectrochim. Acta, Part A*, 1999, **55**, 1585.
50 R. L. A. Haiduke, A. E. Oliveira, N. H. Moreira and R. E. Bruns, *J. Phys. Chem. A*, 2004, **108**, 866.
51 A. B. M. S. Bassi and R. E. Bruns, *J. Chem. Phys.*, 1975, **82**, 3235.
52 R. E. Bruns, *J. Mol. Struct.*, 1975, **26**, 124.
53 P. A. Guadagnini, A. E. Oliveira, R. E. Bruns and B. B. Neto, *J. Am. Chem. Soc.*, 1997, **119**, 4224.

